The Astrophysical Journal, 713:318–324, 2010 April 10 doi:10.1088/0004-637X/713/1/318

RXTE-BASED 35 DAY CYCLE TURN-ON TIMES FOR HERCULES X-1

Denis A. Leahy and Ciprian D. Igna
Department of Physics and Astronomy, University of Calgary, Calgary, AB T2N 1N4, Canada; leahy@ucalgary.ca
Received 2009 December 1; accepted 2010 February 26; published 2010 March 19

ABSTRACT

The 35 day X-ray cycle of Hercules X-1 (Her X-1) has been the subject of intense study since its discovery over 30 years ago. This work summarizes the results of determination of 35 day cycle turn-on (TO) times based on *Rossi X-Ray Timing Explorer* (*RXTE*)/All-Sky Monitor (ASM) observations of Her X-1. We apply a cross-correlation method to the entire (*RXTE*/ASM) Her X-1 database acquired between 1996 February 20 and 2009 December 18. We obtain new TO times for 147 cycles, 94 of which have well-determined times. The results reveal a uniform distribution of TO times with orbital phase. This does not support previous results that suggest TO times cluster around a specific orbital phase, such as 0.2 or 0.7. We also find 35 day cycle lengths ranging from 33.2 days to 36.7 days, and an average cycle length of 34.7 days.

Key words: stars: individual (Her X-1, HZ Her) – stars: neutron – X-rays: binaries

1. INTRODUCTION

HZ Herculis/Hercules X-1, also known as HZ Her/Her X-1, was discovered in 1971 November (Schreier et al. 1972; Tananbaum et al. 1972) and is one of the brightest and most studied low-mass X-ray binary systems to date (e.g., Klochkov et al. 2009; Ji et al. 2009; Leahy 2002, 2003; Scott 1993; Crosa & Boynton 1980; Gerend & Boynton 1976). The system is located at a distance of approximately 6.6 kpc from Earth, has an A7 type (which varies between late A and early B with the orbital phase) main-sequence stellar companion, HZ Her, and a neutron star of approximate masses 2.2 $M_{\odot}$ and 1.5 $M_{\odot}$, respectively (Reynolds et al. 1997). The system is characterized by a great variety of phenomena, such as 1.24 s pulsations, 1.7 day orbital period eclipses, and a 35 day X-ray intensity cycle, and is one of the few to have low interstellar absorption, which makes it feasible for observation and study at various wavelengths (e.g., Leahy 2002, 2003; Scott et al. 2000; Scott & Leahy 1999; Boynton et al. 1980).

The 35 day periodicity in the HZ Her/Her X-1 system was noticed since its discovery (Tananbaum et al. 1972). The 35 day cycle is the best known among the super-orbital periods of X-ray binaries (see, e.g., Foulkes et al. 2010 and Durant et al. 2010 for recent discussions of super-orbital periods). The 35 day cycle is produced by a counterprecessing, tilted, and twisted neutron star accretion disk (Giacconi et al. 1973; Roberts 1974; Petterson 1975; Gerend & Boynton 1976; Becker et al. 1977; Boynton et al. 1980; Scott 1993; Larwood et al. 1996; Maloney et al. 1996; Maloney & Begelman 1997; Scott & Leahy 1999; Wijers & Pringle 1999; Scott et al. 2000; Leahy 2002, 2003, 2004a, 2004b; Klochkov et al. 2006). The cycle consists of a Main High (MH) state that covers phases 0–0.31 and a Short High (SH) state covering the 0.57–0.79 phase interval; the MH and SH states are separated by fainter Low States (LS; Scott & Leahy 1999).

The disk is also responsible for the evolution of the pulse profile and for shadowing and occulting the companion star. The X-ray source is occulted by the outer and inner disk edges. The two-layer disk atmosphere is mainly responsible for the time dependence of the turn-on (TO) of both MH and SH states. However, the X-ray source geometry is likely responsible for the time dependence of the declines of the two states (Leahy 2002).

In this paper, we report the results of a cross-correlation (CC) analysis using the *Rossi X-Ray Timing Explorer* (*RXTE*)/All-Sky Monitor (ASM) observations of HZ Her/Her X-1. We used the entire *RXTE*/ASM database acquired between 1996 February 20 and 2009 December 18. We use an iterative procedure to determine TO times and the average 35 day Her X-1 light curve. For an initial average 35 day light curve we use the ones in Scott & Leahy (1999). Below, we describe the analysis and the resulting TO times and cycle lengths.

2. DATA AND ANALYSIS

The *RXTE*/ASM daily-averaged data for Her X-1 was obtained for the period between 1996 February 20 and 2009 December 18 using the Massachusetts Institute of Technology (MIT) *RXTE* project online database. The daily-averaged data consists of a total of 4783 data points. We use the summed band count rate (1.5–12 keV), shown in Figure 1. The technical details of the ASM detector on board the *RXTE* satellite are covered elsewhere (Levine et al. 1996) along with a comprehensive description of the 35 day X-ray cycle (Scott 1993; Scott & Leahy 1999). The orbital period and period derivative were obtained (Deeter et al. 1991). The 90° mean longitude time, T90 = MJD50086.6390977 dynamical barycentric time (TDB), was used (Scott & Leahy 1999) in order to calculate orbital phase.

We used the CC of the observed ASM count rates with a 35 day cycle average light curve, hereafter referred to as the template, to determine TO times. The times of maxima of the CC function correspond to the best match between the template and the data. The CC function is calculated as the product of the data and the template shifted by a time offset, t_n:

$$F(t_n) = \sum_{k=1}^{K_{\max}} [R_k \times Tem((t_k - t_n)/P_{35})], \qquad (1)$$

where t_n is the time offset with index n, R_k is the observed count rate at time t_k, and $K_{\max} = 4783$ is the number of data points in the *RXTE*/ASM data set. The template $Tem(t/P_{35})$ is defined to be zero for $t/P_{35} < -0.1$ and for $t/P_{35} > 0.9$, so that the sum reduces to the sum over only one cycle of data for any given t_n. We chose a 0.035 d time step, which yields over 145,000 time steps, t_n, and the same number of CC values. The initial average

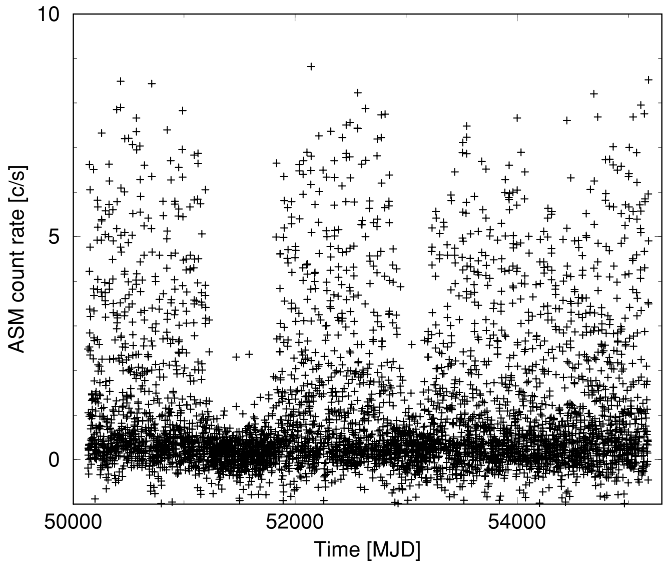

Figure 1. *RXTE*/ASM daily-averaged 2–12 keV count rate vs. time over the period 1996 February 20 to 2009 December 18 used in the current study.

35 day light curve was obtained from those in Scott & Leahy (1999). They were produced by averaging the ASM dwell flux data recorded between 1996 March 2 and 1998 May 12 (Scott & Leahy 1999). The 35 day phase was obtained by using observed TOs of Her X-1 pulsations by the Burst and Transient Source Experiment (BATSE) on the *Compton Gamma-Ray Observatory* (*CGRO*). The 0.2 TO and 0.7 TO light curves of Scott & Leahy (1999) are slightly different. However, because the 35 day light curve of Her X-1 is known to be quite variable, the difference may be caused just by different sampling of the variability (12 0.2 TO cycles and 10 0.7 TO cycles of ASM data were used to produce the 0.2 TO and 0.7 TO light curves). For the current work, the eclipses and dips (e.g., Giacconi et al. 1973) were removed manually from the 0.2 TO and 0.7 TO 35 day average light curves.[1] Then the light curves were smoothed to produce 0.2 TO and 0.7 TO smooth templates. Both templates were fitted with a linear spline in order to turn them into continuous functions.

Preliminary TO times were obtained from the CC function peaks using the initial templates. The average (and standard deviation) of the difference in TO times from 0.2 TO and 0.7 TO initial templates was 0.002 days (and 0.4 days). We compare to the published 22 BATSE TO times (Scott & Leahy 1999): the average (and standard deviation) of the difference with the BATSE TO times is 0.26 days (and 0.67 days). However, four of the cycles (starting near MJD50182, 50601, 50635, and 50808) had gaps in the ASM data of two or more days, and when we omit these cycles the average difference (and standard deviation) with the BATSE TO times is reduced, to 0.21 days (and 0.35 days). We also note that the CC method detected the TO for MJD50670, which was not detected by BATSE (Scott & Leahy 1999).

The initial template was based on only 22 cycles (Scott & Leahy 1999), but we make an improved template using all of the *RXTE*/ASM data, excluding anomalous low states (ALS) and cycles with poor data coverage. The 35 day phases needed to make the new template were obtained using TO times and resulting 35 day cycle lengths[2] from the initial CC runs (we use the average of the TO times from the CCs using the 0.2 TO and 0.7 TO initial templates). An example template is shown in Figure 2. Figure 2 also illustrates the definition of 35 day phase 0 (similar to that of Scott & Leahy 1999): the time that the ASM 2–12 keV count rate rises to 20% of the peak count rate.

To estimate the noise level on the CC function, the CC function was calculated for the template cross-correlated with the ASM count rate errors. The resulting distribution of the 145,000 CC values is shown in Figure 3. From this, we obtain that any value of CC function above 30 is real with 99% confidence level. Figure 4 shows an example CC function versus MJD for the time period MJD51000 to MJD52000 (the CC functions from all 12 CC iterations look similar). This illustrates normal CC values (prior to MJD51200 and after MJD51840) as well as low CC values from the anomalous low state of Her X-1 in between. We see that the anomalous low period gives no real peaks but outside the anomalous low, each 35 day cycle has two real peaks: one where the main peak of the template matches the peak of MH state and one where the main peak matches

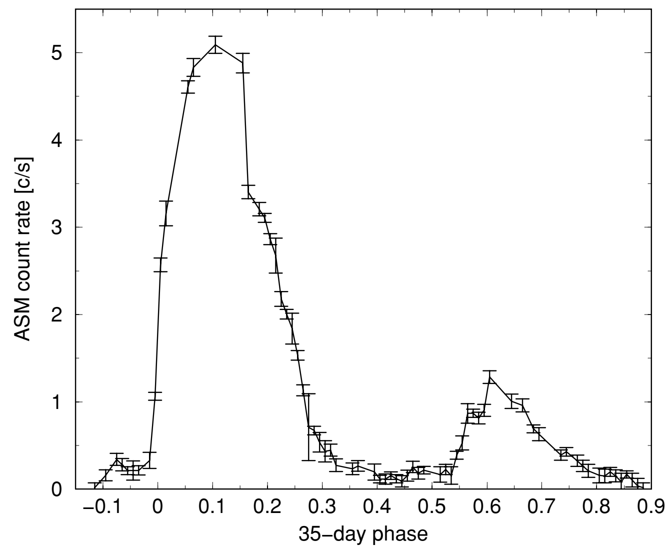

Figure 2. Example of the *RXTE*/ASM X-ray count rate vs. 35 day phase for the smoothed template. For this case, the template was produced using the output TO times and 35 day cycle lengths from iteration 11 of the CC method.

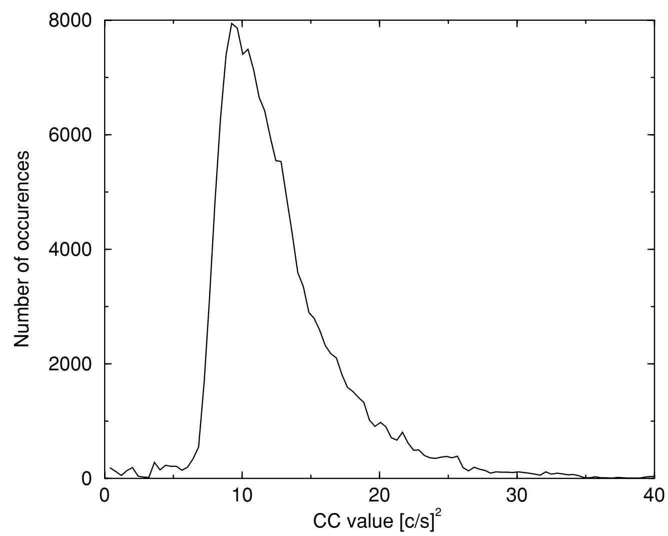

Figure 3. Distribution of CC values for CC of the smooth 35 day cycle template with ASM noise count rates.

[1] They would have biased the CC if not removed, since their occurrence is not at fixed 35 day phase.

[2] We define cycle lengths as the difference in consecutive TO times.

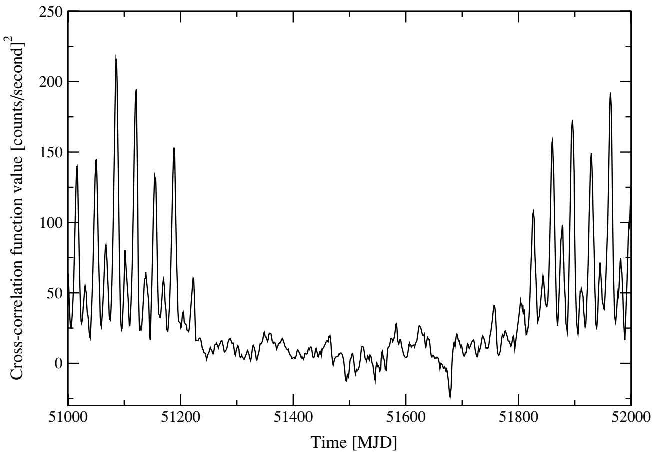

Figure 4. CC function over the MJD51000–MJD52000 interval, which contains the longest *RXTE*/ASM low-count-rate state.

the peak of the SH state. This second peak is not of interest for determining the TO times of the 35 day cycle. The number of significant peaks in the CC function (number of TOs detected) is 125. We note that the first and last cycles are incomplete in the ASM data (those with TO near MJD50111 and 55177) and the first cycle does not give a significant peak. Also, the cycles with TOs between MJD51255 and 51724 and between MJD 52945 and 53124 occur during anomalous low states and are not detected by the CC method. Upon detailed inspection of the ASM data, a number of 35 day cycles have ASM data gaps of two or more days which occur during MH. As a result of the data gap, there is a shift in the time of peak of the CC function, thus we do not include these cycles in the analysis. The 33 cycles with data gaps are those listed in Table 1 marked as incomplete (by Inc.) in the third column. This leaves 94 cycles. Eight of these cycles (with TO near MJD 50356, 50704, 51894, 52033, 52243, 52454, 52595, and 53575) have TO well constrained with *RXTE*/Proportional Counter Array (PCA) data,[3] so we use TO times from the PCA observations for these cycles, leaving 86 cycles with TO times to determine using the CC method. In summary, we find new TO times for the 86 cycles (eight of the 94 cycles with good data coverage are better determined by PCA archival data) and estimate TO times for the remaining cycles.

We carry out the following analysis to determine TO times and cycle lengths and to estimate their errors. We iterate on the procedure of producing a template and finding TO times as follows. As noted above, we created a template from the 94 good cycles using the TO times and cycle lengths from the initial CC runs. Dips are removed from this template and linear interpolation used to obtain a smooth template function. The new template is used as input to the CC calculation to determine iteration 2 TO times and cycle lengths for the 86 cycles. We add the TO times from the eight cycles determined by the PCA data. This allows binning the 94 cycles of ASM data in 35 day phase to produce an iteration 2 35 day template. The iteration 2 template is used as input to the CC calculation to produce iteration 3 TO times and 35 day phases. This is repeated up to iteration 12.

Examination of the differences of TO times from iterations 1 to 12 shows improvement from iteration 1 to iteration 2, then followed by fluctuations (in both TO times and template). To

3 The details of the *RXTE*/PCA analysis will be covered in a separate publication.

Table 1
RXTE/ASM 35 day X-ray Cycle TO Times, Cycle Lengths, and Orbital Phases

Cycle[a]	MJD TO	Length (days)	TO Orbital Phase[b]	TO Error (days)[c]
1	50110.9	35.3	Inc.	
2	50146.2	35.3	0.0	0.1
3	50181.5	35.3	Inc.	
4	50216.8	35.1	0.5	0.3
5	50251.9	34.1	0.2	0.2
6	50286.0	35.0	0.2	0.2
7	50320.9	35.2	0.8	0.3
8	50356.1	34.3	0.5	PCA
9	50390.4	34.8	0.7	0.4
10	50425.2	35.4	0.1	0.2
11	50460.6	35.9	0.9	0.3
12	50496.5	34.5	0.1	0.6
13	50531.0	35.1	0.4	0.2
14	50566.1	34.6	0.0	0.2
15	50600.7	34.6	Inc.	
16	50635.2	34.6	Inc.	
17	50669.8	34.6	Inc.	
18	50704.3	34.9	0.3	PCA
19	50739.2	34.0	0.8	0.4
20	50773.2	34.5	0.8	0.4
21	50807.7	34.5	Inc.	
22	50842.2	35.2	0.4	0.1
23	50877.4	35.2	Inc.	
24	50912.6	34.8	0.8	0.4
25	50947.4	34.9	0.3	0.4
26	50982.3	34.1	0.8	0.7
27	51016.4	33.8	0.8	0.5
28	51050.2	34.6	0.7	0.7
29	51084.8	34.6	Inc.	
30	51119.4	34.6	Inc.	
31	51154.1	34.6	Inc.	
32	51188.7	33.8	0.2	0.5
33	51222.5	33.4	0.1	0.3
34	51255.9	33.4	Low	
35	51289.3	33.4	Low	
36	51322.7	33.4	Low	
37	51356.1	33.4	Low	
38	51389.5	33.4	Low	
39	51422.9	33.4	Low	
40	51456.3	33.4	Low	
41	51489.7	33.4	Low	
42	51523.1	33.4	Low	
43	51556.5	33.4	Low	
44	51589.9	33.4	Low	
45	51623.3	33.4	Low	
46	51656.7	33.4	Low	
47	51690.1	33.4	Low	
48	51723.5	33.4	Low	
49	51756.9	34.4	0.4	0.2
50	51791.3	34.4	Inc.	
51	51825.7	34.4	Inc.	
52	51860.0	34.6	0.1	0.2
53	51894.6	34.6	0.4	PCA
54	51929.2	34.6	Inc.	
55	51963.8	34.6	Inc.	
56	51998.4	34.6	Inc.	
57	52033.0	35.2	0.8	PCA
58	52068.1	34.9	0.5	0.2
59	52103.0	35.8	1.0	0.2
60	52138.8	36.1	0.1	0.2
61	52175.0	34.1	0.3	0.2
62	52209.0	34.1	Inc.	
63	52243.1	35.2	0.4	PCA
64	52278.3	35.2	Inc.	
65	52313.5	35.2	Inc.	
66	52348.8	35.1	0.5	0.3

Table 1
(Continued)

Cycle[a]	MJD TO	Length (days)	TO Orbital Phase[b]	TO Error (days)[c]
67	52383.9	35.1	Inc.	
68	52419.0	35.2	0.9	0.2
69	52454.2	35.8	0.5	PCA
70	52490.0	35.1	0.6	0.3
71	52525.1	34.3	0.2	0.2
72	52559.4	35.7	0.4	0.3
73	52595.1	35.2	0.4	PCA
74	52630.3	35.2	Inc.	
75	52665.5	35.2	Inc.	
76	52700.7	35.2	Inc.	
77	52735.9	35.4	0.2	0.2
78	52771.3	35.3	0.1	0.2
79	52806.6	35.3	Inc.	
80	52841.9	34.8	0.6	0.4
81	52876.7	33.2	0.1	0.5
82	52909.9	35.6	0.6	0.5
83	52945.5	35.6	Low	
84	52981.2	35.6	Low	
85	53016.8	35.6	Low	
86	53052.5	35.6	Low	
87	53088.1	35.6	Low	
88	53123.8	35.6	Low	
89	53159.4	34.4	0.3	0.4
90	53193.9	33.2	0.6	0.3
91	53227.1	35.8	0.1	0.3
92	53262.9	34.1	0.2	0.4
93	53297.0	34.2	0.2	0.2
94	53331.1	34.2	Inc.	
95	53365.3	34.2	Inc.	
96	53399.5	35.3	0.5	0.3
97	53434.8	34.7	0.3	0.2
98	53469.4	34.7	Inc.	
99	53504.1	34.9	0.1	0.2
100	53539.0	35.7	0.6	0.5
101	53574.8	35.3	0.6	PCA
102	53610.0	35.0	0.4	0.2
103	53645.0	34.8	0.9	0.2
104	53679.8	34.8	Inc.	
105	53714.6	34.4	0.9	0.4
106	53748.9	34.6	0.1	0.2
107	53783.5	34.4	0.4	0.2
108	53817.9	35.0	0.7	0.1
109	53852.9	33.8	0.2	0.1
110	53886.7	36.7	0.1	0.5
111	53923.3	34.9	0.7	0.3
112	53958.3	35.8	0.2	0.1
113	53994.1	35.0	0.3	0.1
114	54029.0	35.0	Inc.	
115	54064.0	34.9	0.4	0.1
116	54098.9	34.4	0.9	0.1
117	54133.3	34.8	0.1	0.4
118	54168.1	34.7	0.6	0.2
119	54202.8	33.3	0.0	0.3
120	54236.1	35.0	0.6	0.3
121	54271.1	34.6	0.2	0.1
122	54305.7	35.3	0.6	0.4
123	54340.9	33.4	0.3	0.2
124	54374.4	34.4	0.9	0.5
125	54408.8	34.1	0.2	0.2
126	54442.8	35.2	0.2	0.2
127	54478.1	34.3	0.9	0.2
128	54512.4	34.4	0.1	0.3
129	54546.8	35.9	0.4	0.2
130	54582.7	34.3	0.5	0.3
131	54617.0	35.3	0.7	0.2
132	54652.2	35.2	0.4	0.6

Table 1
(Continued)

Cycle[a]	MJD TO	Length (days)	TO Orbital Phase[b]	TO Error (days)[c]
133	54687.5	34.7	0.1	0.3
134	54722.2	33.9	0.5	0.2
135	54756.1	36.0	0.4	0.2
136	54792.0	34.9	0.6	0.6
137	54827.0	34.6	0.1	0.1
138	54861.5	35.4	0.5	0.5
139	54896.9	34.9	0.3	0.4
140	54931.8	36.4	0.8	0.3
141	54968.2	34.0	0.2	0.2
142	55002.2	35.4	0.2	0.2
143	55037.6	34.8	0.0	0.4
144	55072.4	34.8	Inc.	
145	55107.2	34.8	Inc.	
146	55142.0	34.8	Inc.	
147	55176.8	34.8	Inc.	

Notes.
[a] The cycle count given here assumes that the ALS between MJD51255 and MJD51756 consists of 16 cycles (15 undetected TOs). For the other possibility of 15 cycles (14 undetected TOs), the cycle count for cycles 49–147 would each be reduced by 1, and the cycle length for the 15 cycles in the anomalous low would increase from 33.4 days to 35.63 days.
[b] TO orbital phase is not well determined for cycles with data gaps, marked by Inc. (for incomplete), or for cycles during ALSs, marked low.
[c] The error in TO time is not given for cycles with data gaps or cycles during ALSs; for cycles with TO determined by *RXTE*/PCA data, marked PCA, the error is small, <0.1 days.

obtain our final values for TO times, we average the TO times from iterations 2 through 12, omitting the first iteration. For each of 86 individual cycles, we calculate the standard deviation of TO times from iterations 2 through 12. The standard deviations are used as an estimate of the error in TO time and are given in Column 4 of Table 1. Most cycles are seen to have TO times with a standard deviation of 0.2–0.5 days, but a few have larger standard deviations up to 0.7 days. We think that the reason for the difference in accuracy of determination of TO times, measured by standard deviation, is the different ASM sampling of the different 35 day cycles. For some cycles, one or more data points may fall in the middle of an eclipse or major dip.

We carried out a similar CC analysis using the ASM dwell data. However, the larger errors in the dwell count rates resulted in the detection of much fewer 35 day cycles, with more uncertain TO times, compared to the analysis done with the ASM daily average data.

3. RESULTS AND DISCUSSION

This study contains the largest record of TOs for the HZ Her/Her X-1 system to date. We have *RXTE*/ASM data coverage of a total of 147 cycles. Of these, 125 TOs were detected with the CC method, with the remaining cycles during anomalous low states. The 125 TOs include eight cycles with *RXTE*/PCA data coverage, which determines the TO times for those cycles. Thirty-three cycles have significant ASM data gaps which preclude accurate determination of TO time. This leaves 86 cycles for which we have applied the CC method to determine TO times. We apply the CC method iteratively, where we construct a new 35 day light-curve template from the ASM data using the TO times from the CC method and use this template as input for the next iteration. The iterative method reaches a limit of accuracy which is probably to be caused by the limitations of the *RXTE*/ASM data.

3.1. *New Estimate of the 35 day Cycle Length*

Table 1 gives the TO times and cycle lengths for the entire *RXTE*/ASM data set studied here. It includes the 86 cycles with good ASM data coverage analyzed by the CC method above. For these, the error in TO time from the CC analysis is also listed. The eight cycles with TO times determined by *RXTE*/PCA data are also listed. For these 94 cycles, cycle lengths can be determined when consecutive TOs are found. The average cycle length of these cycles is 34.5 days, with a maximum of 36.7 days and minimum of 33.2 days.

The 33 cycles with ASM data gaps are spread throughout the *RXTE*/ASM data set. In most cases there were adjacent cycles with good TO times, in four cases there were three consecutive cycles with ASM data gaps, and in one case four consecutive cycles with data gaps. We examined the TO times determined for these cycles with the CC method, but found that the data gaps induced errors up to 6 days. Thus, we use linear interpolation to determine the TO times for these cycles, i.e., for one missing TO we assume that the TO time occurs midway between the two measured TOs. This yields reasonable cycle lengths for all interpolated cycles. We have checked the TO times for all cycles in Table 1 against the ASM light curves and find that the TO times correspond to rise of the 35 day cycle, as they should. Additionally, we verified that the interpolated cycles agree well with the data for the cycles with data gaps, whereas the CC peak times can be off by several days for these cycles.

For the cycles that fall during ALS, we measure the gaps between the measured TO times for the last cycle before the ALS and first cycle after the ALS. For the longer ALS (ALS1) between the TOs at MJD 51222.5 and MJD 51756.9, the gap is 534.4 days. From the distribution of measured cycle lengths, we find that there is either a cycle count of $N_{\mathrm{ALS1}} = 15$ (14 missing TOs) or $N_{\mathrm{ALS1}} = 16$ (15 missing TOs) in the gap. Fourteen or 17 cycles give cycle lengths too long or too short to be consistent with any cycle length ever measured for Her X-1. The resulting average cycle length for this ALS is 33.4 days for 16 cycles or 35.6 days for 15 cycles. For the shorter ALS from MJD 52909.9 to MJD 53159.4, the gap length is 249.5 days.[4] This gap can only be fit with seven cycles (six missing TOs) of length 35.6 days, as either six or eight cycles would give unreasonable cycle lengths (41.6 days and 31.1 days, respectively). Figure 5 shows the cycle lengths we find plotted against MJD of TO, assuming 16 cycles during ALS1. For the case $N_{\mathrm{ALS1}} = 15$, the only change in the plot would be that the cluster of points near MJD51500 would move up to a cycle length of 35.6 days. In either case the longest cycle is cycle 110 (36.7 days), which is constrained by measured TOs at both ends of that cycle.

Still & Boyd (2004) carried out an observed-minus-calculated (O–C) analysis for MH states, using a reference 35 day cycle length of 34.79 days, and inferred an increase in O–C during the long ALS. On the other hand, the long ALS cycle lengths were inferred to be shorter than average (34.85 days) by Staubert et al. (2006) also with an O–C analysis (with reference cycle length of 34.85 days). The ambiguity in cycle count for this ALS, which we find, does not allow one to choose between the two alternatives.

As a result of our analysis, we know the cycle count over the whole period of *RXTE*/ASM observations with an error of one: from the first well-measured TO time at MJD50146.2 to the last well-measured TO time at MJD55037.6, the cycle count is 141 or 140 (using 16 cycles or 15 cycles during ALS1). The resulting average 35 day cycle length is then determined, with the main error of 0.24 day from the uncertainty in cycle count and the remaining error from the uncertainties in first TO time and last TO time:

$$P_{35,\mathrm{avg.}} = 34.691 \pm 0.005\,\mathrm{day}, \quad \text{if } \mathrm{N_{ALS1}} = 16 \qquad (2)$$

$$= 34.939 \pm 0.005\,\mathrm{day}, \quad \text{if } \mathrm{N_{ALS1}} = 15. \qquad (3)$$

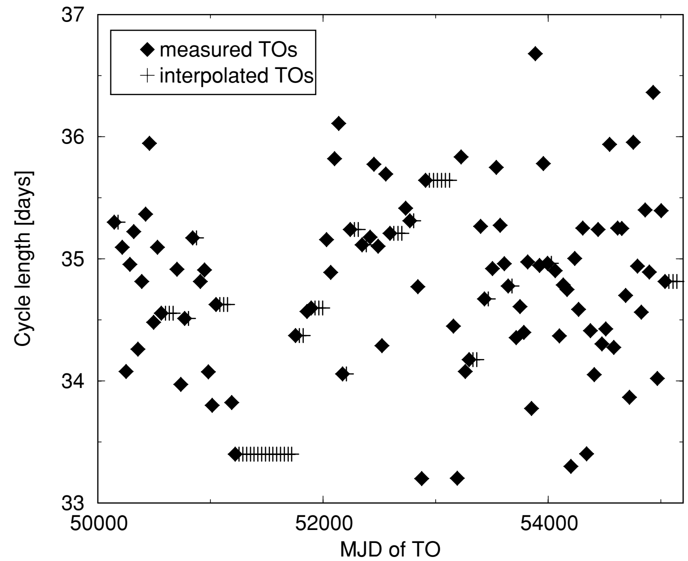

Figure 5. Derived 35 day cycle lengths as a function of MJD of TO. Measured TOs are plotted as diamonds, interpolated TOs are plotted as + symbols.

3.2. *The Orbital Phase of the 35 day Cycle TO*

The 35 day cycle starts with a sharp X-ray TO to the MH state. Many observed TOs over the past 30 years were noted to cluster around 0.2 or 0.7 orbital phase (Giacconi et al. 1973; Becker et al. 1977; Davison & Fabian 1977; Crosa & Boynton 1980; Klochkov et al. 2006). Zero orbital phase was set at the moment of mid-eclipse of the neutron star by its companion. However, these studies are based only on several months of observations (including Crosa & Boynton 1980, which summarizes several short-observation studies that extend, with extensive data gaps, over a long period of time). We note that two studies (Scott & Leahy 1999 and Klochkov et al. 2006) assumed TO times at orbital phase of 0.2 or 0.7 and rounded the TO times to the nearest time of orbital phase 0.2 or 0.7. This results in the alignment of eclipses for all 35 day cycles for each (0.2 TO or 0.7 TO) set of cycles.

Figure 6 shows the 35 day cycle lengths versus orbital phase. We plot only the 94 cycles for which the TOs are determined. An interesting feature that can be seen from Figure 6 is that the CC method can identify TOs even if they occur during eclipses, which cannot be achieved by methods based on start of X-ray pulsations. The lack of any trend and lack of clustering of TOs at any specific orbital phases is seen in Figure 6: the TOs are spread out over orbital phase. This also shows no preference for any cycle length with orbital phase of TO. We have calculated the cumulative probability distribution and applied the Kolmogorov–Smirnov (K–S) test: it gives results consistent with the uniform distribution (K–S statistic of 0.19 or probability of 0.06), but not consistent with two values of

[4] This period includes one detected cycle at MJD52945, but this cycle has data gaps, so we use the previous detected TO at MJD52909.8 and include cycle 83 (Table 1) in the ALS gap for the purpose of calculating cycle lengths.

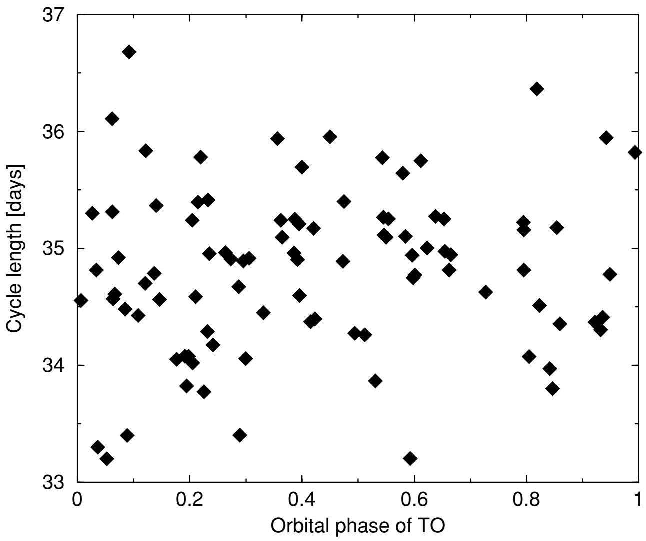

Figure 6. 35 day cycle length plotted against orbital phase of TO.

TO at 0.2 and 0.7 (K–S statistic of 0.41 with probability less than 10^{-6}). However, the errors in phase values are significant here, typically 0.4 days or 0.24 days in orbital phase, which is not taken into account in the K–S test, so we apply another statistical test which includes errors in phase. We divide the TOs into two sets: those with TO before orbital phase 0.5 and those with TO after phase 0.5. For the first group, we find the reduced χ^2 statistic comparing the phases to a single phase of 0.2 for TO is 51, highly improbable. For the second group, the reduced χ^2 statistic comparing to a single phase of 0.7 for TO is 78, also highly improbable.

Thus, we find no evidence for the association of 35 day cycle TOs with orbital phases 0.2 or 0.7, nor any other particular orbital phase. However, we point out that the CC method measures the timing of the best match between the 35 day light-curve template and the ASM data. Thus, it is still possible, but we consider it unlikely that the TO defined by the first detection of pulsations from the neutron star occurs at particular orbital phases, but that the TO defined by the 35 day light curve is not related to orbital phase.

3.3. Correlation of 35 day Cycle Length with Flux

For each 35 day cycle, we calculate the cycle-average ASM count rate and its error. In Figure 7, the 35 day cycle lengths are plotted against cycle-average ASM count rate, with the values for well-determined cycle lengths plotted as diamond symbols and those for interpolated cycle lengths plotted as plus symbols. Using only well-determined cycle lengths, the Pearson's r correlation coefficient is 0.44, indicating a correlation. A χ^2 fit of a linear relation of ASM count rate versus cycle length[5] results in a poor fit (χ^2 per degree of freedom of 19), caused by scatter much larger than the error bars. However, the slope of 0.24 cs^{-1} per d is highly significant—the fit with zero slope has a much higher χ^2 (χ^2 per degree of freedom of 28). The measured slope is consistent with the long ALS having an average cycle length of 33.4 days but not consistent with the larger value of 35.6 days. Thus, we prefer to use the shorter cycle length for the long ALS. We note that Staubert et al. (2006) have shown that the 35 day cycle length correlates with pulse period variations:

[5] Because the relative errors on count rate are larger than for cycle length and count rate errors dominate, it is better to fit count rate vs. cycle length rather than cycle length vs. count rate.

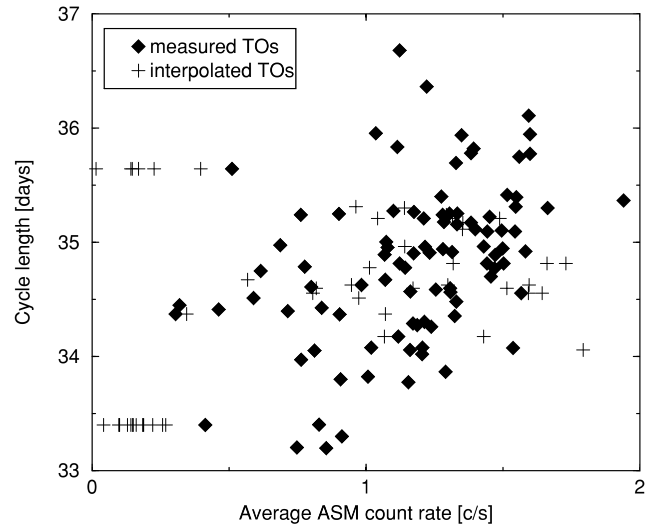

Figure 7. 35 day cycle length plotted against 35 day cycle average ASM count rate. Measured TOs are plotted as diamonds, interpolated TOs are plotted as + symbols.

shorter cycle length is associated with spin-down. Spin-down is expected to be related to decreased X-ray luminosity, caused by the increasing radius of the magnetospheric boundary with reduced mass accretion rate. The correlation found here is consistent with this.

4. CONCLUSIONS

The 35 day X-ray cycle is a well-known feature of Her X-1, and is produced by the counterprecessing, tilted and twisted accretion disk of the neutron star. However, our knowledge of the 35 day cycle's properties is still incomplete. The (*RXTE*)/(ASM) has been continuously monitoring the HZ Her/Her X-1 binary star system since 1996 February. In this study, we have used a CC method to find the largest set of TO times for Her X-1 to date. We find a 35 day cycle length of 34.7 or 34.9 days, for the two possible cases of cycle count in the long ALS, with a range of cycle lengths from 33.2 to 36.7 days.

The start of the 35 day X-ray cycle (zero for 35 day phase), also known as the X-ray TO, was expected to be concentrated around orbital phases 0.2 and 0.7, based on several previous observations of start of X-ray pulsations. In contrast, the TO times measured here, which include 94 TOs from over 13 years of continuous light-curve data, occur at all orbital phases.

The ASM daily-averaged and dwell data were obtained from the *RXTE*/ASM teams at the MIT Kavli Institute for Astrophysics and Space Research and at the *RXTE* Science Operations Facility (SOF) and Guest Observer Facility (GOF) at NASA's Goddard Space Flight Centre (GSFC). This work was supported by the Natural Sciences and Engineering Research Council of Canada.

REFERENCES

Becker, R. H., Boldt, E. A., Holt, S. S., Pravdo, S. H., Rothschild, R. E., Serlemitsos, P. J., Smith, B. W., & Swank, J. H. 1977, ApJ, 214, 879
Boynton, P. E., Crosa, L. M., & Deeter, J. E. 1980, ApJ, 237, 169
Crosa, L., & Boynton, P. E. 1980, ApJ, 235, 999
Davison, P. J. N., & Fabian, A. C. 1977, MNRAS, 178, 1P
Deeter, J. E., Boynton, P. E., Myamoto, S., Kitamoto, S., Nagase, F., & Kawai, N. 1991, ApJ, 383, 324
Durant, M., Cornelisse, R., Remillard, R., & Levine, A. 2010, MNRAS, 401, 355

Foulkes, S. B., Haswell, C. A., & Murray, J. R. 2010, MNRAS, 401, 1275

Gerend, D., & Boynton, P. E. 1976, ApJ, 209, 562

Giacconi, R., Gursky, H., Kellog, E., Levinson, R., Schreier, E., & Tananbaum, H. 1973, ApJ, 184, 227

Ji, L., Schulz, N., Nowak, M., Marshall, H. L., & Kallman, T. 2009, ApJ, 700, 977

Klochkov, D. K., Shakura, N. I., Postnov, K. A., Staubert, R., Wilms, J., & Ketsaris, N. A. 2006, Astron. Lett., 32, 804

Klochkov, D., Staubert, R., Postnov, K., Shakura, N., & Santangelo, A. 2009, A&A, 506, 1261

Larwood, J. D., Nelson, R. P., Papaloizou, J. C. B., & Terquem, C. 1996, MNRAS, 282, 597

Leahy, D. A. 2002, MNRAS, 334, 847

Leahy, D. A. 2003, MNRAS, 342, 446

Leahy, D. A. 2004a, MNRAS, 348, 932

Leahy, D. A. 2004b, Astron. Nachr., 325, 205

Levine, A., Bradt, H., Cui, W., Jernigan, J., Morgan, E., Remillard, R., Shirley, R., & Smith, D. 1996, ApJ, 469, L33

Maloney, P. R., & Begelman, M. C. 1997, ApJ, 491, L43

Maloney, P. R., Begelman, M. C., & Pringle, J. E. 1996, ApJ, 472, 582

Petterson, J. A. 1975, ApJ, 201, L61

Reynolds, A. P., Quaintrell, H., Still, M. D., Roche, P., Chakrabarty, D., & Levine, S. E. 1997, MNRAS, 288, 43

Roberts, W. J. 1974, ApJ, 187, 575

Schreier, E., Levinson, R., Gursky, H., Kellogg, E., Tananbaum, H., & Giacconi, R. 1972, ApJ, 172, L79

Scott, D. M. 1993, PhD thesis, Univ. of Washington

Scott, D. M., & Leahy, D. A. 1999, ApJ, 510, 974

Scott, D. M., Leahy, D. A., & Wilson, R. B. 2000, ApJ, 539, 392

Staubert, R., Schandl, S., Klochkov, D., Wilms, J., Postnov, K., & Shakura, N. 2006, in AIP Conf. Proc. 840, the Transient Milky Way: A Perspective for Mirax, ed. J. Braga, F. D'Amico, & R. E. Rothschild (Melville, NY: AIP), 65

Still, M., & Boyd, P. 2004, ApJ, 606, L135

Tananbaum, H., Gursky, H., Kellogg, E. M., & Levinson, R. 1972, ApJ, 174, L143

Wijers, R. A. M. J., & Pringle, J. E. 1999, MNRAS, 308, 207